PHYSICAL REVIEW C VOLUME 17, NUMBER 3 MARCH 1978

Giant $E1$ resonance in ^{16}O observed with the reaction $^{15}N(p,\gamma_0)^{16}O$

W. J. O'Connell* and S. S. Hanna
Department of Physics, Stanford University, Stanford, California 94305

(Received 16 September 1977)

The giant electric dipole resonance based on the ground state (0^+) of ^{16}O has been studied with the reaction $^{15}N(p,\gamma_0)^{16}O$ from $E_p = 8.6$ to 18.0 MeV ($E_\gamma = 20.2$ to 29.0 MeV). The $E1$ strength in (γ,p_0) is concentrated between $E_\gamma = 20$ and 29 MeV where it exhausts about 15% of the $E1$ sum rule. Major peaks are displayed at 22.2 and 25.0 MeV and secondary structure at 21.0, 22.9, and in the 24 MeV region. The angular distributions indicate predominantly dipole radiation and are fairly constant over the entire range, except in the region of the secondary peaks where the coefficient of $P_2(\cos\theta)$ displays striking interference effects. This behavior supports the suggestion that these structures are due to interference between more complex states and the simple particle-hole configurations of the $E1$ resonance. The value of the coefficient of $P_2(\cos\theta)$ can be used to restrict greatly the allowed configurations of the p_0 channel—the solution is predominantly either $d_{3/2}$ wave or $s_{1/2}$ wave. The presence of terms in $P_1(\cos\theta)$ and $P_3(\cos\theta)$ indicates significant $E2$ strength which increases above the $E1$ resonance. Data are also presented on the reactions $^{15}N(p,\gamma_1-\gamma_4)^{16}O$ and $^{15}N(p,\alpha\gamma_{15.1})^{12}C$.

[NUCLEAR REACTION $^{15}N(p,\gamma_0)$, $E = 8.6$–18.0 MeV; measured $\sigma(E;E_\gamma,\theta)$. Deduced properties γ_0 giant resonance of ^{16}O. 99.3% enriched ^{15}N gas target.]

I. INTRODUCTION

The giant electric dipole resonance (GDR) is a striking phenomenon lying in the nuclear continuum that has proved amenable to treatment by collective or shell-model theories. The experimental study is greatly simplified by the use of gamma radiation which selectively excites the dipole oscillations of a nucleus. The magnetic dipole resonance is strongly excited but lies at a lower energy, while the electric quadrupole strength, although observable, is much less intense in gamma-ray excitation.

In the light nuclei the GDR often breaks up into well defined intermediate structures which provide a challenge for the various shell-model theories. Since the "closed-shell" nucleus ^{16}O displays prominent but fairly simple structure in its GDR, it has been a testing ground and has led to many developments and new ideas in photonuclear research. Thus, the simple particle-hole (p-h) shell-model treatment[1] with collective enhancement and elevation of the transition strength,[2,3] the extension to continuum states,[4-6] the attribution of additional structure to interference with multiparticle-multihole states[7,8] or to correlations in the ^{16}O ground state,[9,10] the application of electron scattering and μ or π capture,[11-14] and a description in terms of the collective model,[15] successful in heavier nuclei, have all been applied to ^{16}O.

On the experimental side, the GDR of ^{16}O has been investigated in many reactions. The intermediate structures are clearly seen in the total gamma absorption cross section,[16,17] but are more sharply visible in the separate decay channels of the reaction such as (γ,n_0),[18-21] (γ,p_0),[22,23] or its inverse (p,γ_0)[24,25] which is measured in the present work. The decay of the giant resonance state into the different single nucleon decay channels,[26] (γ,n_i) and (γ,p_i), provides additional tests for the various theoretical models, while decays into the complex particle channels, as observed in the inverse reactions $^{12}C(\alpha,\gamma)^{16}O$,[27,28] $^{13}C(^3He,\gamma)^{16}O$,[29] and $^{14}N(d,\gamma)^{16}O$,[30] have been interpreted in terms of multiparticle-multihole states.[7] Finally, several general properties of the GDR, such as the near-constancy of the angular distributions of the (γ,p_0) channel,[31,32] the interference with quadrupole strength observed by means of the angular distributions,[23,33,34] and the relationship to the GDR's in the neighboring nuclei[35-37] have been studied in ^{16}O.

The yields and angular distributions of the reaction $^{15}N(p,\gamma_0)^{16}O$ have been measured with good energy resolution from E_p = 1.0 to 14 MeV (E_γ = 13 to 25 MeV) by Tanner et al.[24] For the reaction $^{16}O(\gamma,p_0)^{15}N$ the yields and angular distributions have been studied by Baglin and Thompson[22] between E_γ = 20.5 and 30 MeV and by Frederick et al.[23] between E_γ = 21 and 32 MeV. The present work, covering the range E_p = 8.6 to 18 MeV (E_γ = 20 to 29 MeV), extends the high-resolution study of $^{15}N(p,\gamma_0)^{16}O$ to higher energies and measures the angular distributions in finer energy intervals and with better statistics in order to obtain more detailed information on the nature of structure in the GDR of ^{16}O.

II. EXPERIMENTAL PROCEDURE

The proton beam from the Stanford FN tandem Van de Graaff accelerator passed

through a target cell containing ^{15}N gas and was stopped in a Faraday cup. The γ-rays from the reaction were detected by the Stanford 24 × 24 cm NaI γ-ray spectrometer,[38] which is provided with collimation and shielding and mounted on a rotating platform.

The gas target cell, made of stainless steel, had a thin cylindrical wall 4 cm in diameter and an entrance and an exit window 5 cm apart. The windows were made of Mo foil 2.54×10^{-4} cm (2.59 mg/cm^2) thick. The cell is suspended concentrically by a tube in a 20 cm diameter scattering chamber. The tube leads to a gas handling system provided for pumping out the chamber (through a tube connected to the beam tube) and for introducing the target gas and measuring its pressure. The ^{15}N gas, 99.3% pure, was stored in a glass bottle containing molecular sieve granules (manufactured by Linde Division, Union Carbide Co.), which absorbed the gas. When heated these granules released the gas to the target cell; when cooled (by surrounding the bottle with liquid nitrogen) they readsorbed nearly all the gas. With this system the same ^{15}N gas was used over a period of two years without noticeable contamination and with very little loss.

Proton beam currents of 30 to 50 nA were used at the lower bombarding energies and these were decreased to 10 to 25 nA between 17 and 18 MeV. The limiting factor was the counting rate in the NaI detector, the acceptable limit being about 5×10^4 counts/sec mainly due to low energy gamma rays. In order to minimize background in the detector the beam was focused so as to pass through a 3 mm aperture placed 1 m in front of the target and then through the gas cell and into the Faraday cup 5 m beyond the target. The gas target cell, scattering chamber, and Faraday cup were each electrically isolated and their currents were monitored. Since electrons are ejected from the gas-cell windows by the proton beam, in a typical run there were 30 nA of current from the Faraday cup, 7 nA from the gas cell, and -7 nA from the target chamber, with a net current of less than 1 nA from the cell and chamber combined. Thus, the error in the current integration can be estimated at less than 1 part in 30 or better than 3%.

The operation of the NaI spectrometer is described in detail in Ref. 38. The "accepted" spectrum consists of those pulses from the NaI crystal that are unaccompanied by pulses in the anticoincidence shield surrounding the crystal, while the "rejected" spectrum consists of pulses rejected by events in the shield. The total (accepted plus rejected) efficiency of the detector for γ-rays entering the collimator is about 96% for E_γ = 22 MeV. The lineshape of the accepted spectrum for the ^{15}N(p,γ_0) radiation was determined at several energies between E_γ = 21 and 29 MeV and checked with lineshapes from ^{11}B(p,γ)^{12}C and D(d,γ)^{4}He observed under similar conditions. If the peak region in the accepted spectrum is taken from 10% below to 5% above the peak maximum, the ratio of the peak counts (accepted) to total counts (accepted plus rejected) decreases gradually from 0.40 at 21 MeV to 0.30 at 29 MeV. The uncertainty in this trend is about ± 5%. The systematic error in determining the counts in the total lineshape (accepted plus rejected) may be as large as ± 15% owing chiefly to the uncertainty in extrapolating the low-energy tail of the lineshape.

The γ-ray spectra from ^{15}N(p,γ_0)^{16}O were analyzed by fitting them with the standard lineshapes discussed above by means of a least-squares computer program. The changes in lineshape and peak efficiency of the detector with energy were taken into account in determining the absolute yields.

A typical set of spectra from ^{15}N(p,γ) is shown in Fig. 1. In the upper half are shown runs taken at E_p = 10.8 MeV with ^{15}N gas in and out of the target cell for the same integrated current. The cut-off at low energy is due to the anti-pileup circuit in the electronic circuitry of the spectrometer. The highest energy peak is due to the ground state transition from ^{15}N(p,γ_0)^{16}O. The peak near channel 130 is from the 12.71 MeV γ-ray from ^{15}N(p,αγ)^{12}C just above its production threshold. The spectrum from the empty cell shows no background in the vicinity of the γ_0 peak of ^{16}O. The higher counts in this spectrum are due to Mo(p,γ) reactions in the windows of the gas cell. At the bottom of the figure is the rejected spectrum from ^{15}N(p,γ), the counterpart to the uppermost spectrum in the figure. It can be seen that removing the rejected pulses improves the resolution and greatly reduces the cosmic-ray background, which simplifies the analysis;

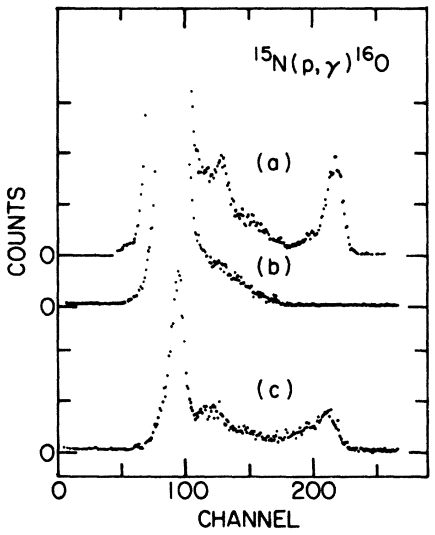

FIG. 1. Spectra obtained from ^{15}N(p,γ)^{16}O at E_p = 10.8 MeV. (a) Full spectrum of all pulses recorded by the NaI detector with ^{15}N gas in cell. (b) Same with cell empty. (c) Spectrum of pulses rejected by the anticoincidence shield.

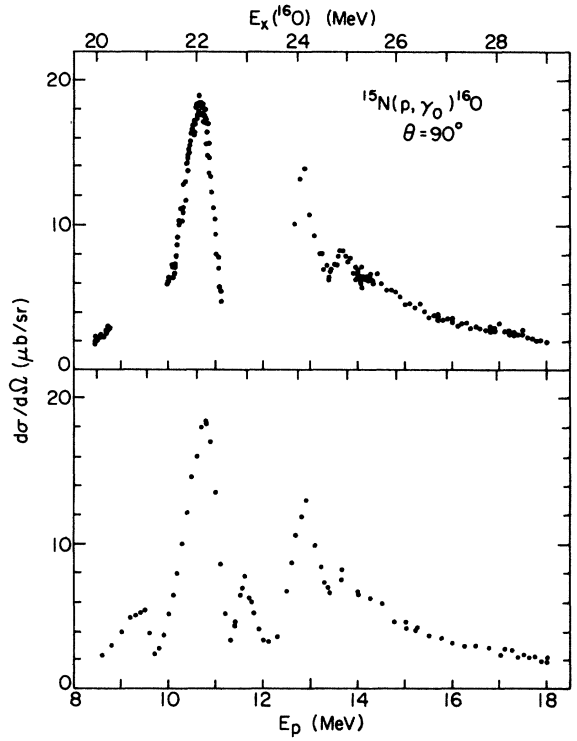

FIG. 2. The 90° yield of $^{15}N(p,\gamma_0)^{16}O$. Top: Measurements taken over selected areas to search for intermediate and fine structure. Bottom: Yields extracted from the angular distribution measurements. The proton energy scale here and in subsequent figures is corrected for the energy loss in the entrance foil of the cell.

but of course the rejected events must be included in computing the absolute cross sections as discussed above.

The 90° yield of $^{15}N(p,\gamma_0)^{16}O$ was measured from E_p = 12.7 to 18.0 MeV in 100 keV steps (some 50 keV steps) at a gas cell pressure corresponding to a target thickness of the order of 40 keV; from E_p = 10.0 to 11.2 MeV in 10 or 20 keV steps with a target thickness of about 15 keV; and from E_p = 8.45 to 8.78 MeV and 13.98 to 14.30 MeV in 20 to 25 keV steps with a target thickness also of about 15 keV. The target entrance window introduced a beam energy loss of about 57 keV at E_p = 10 MeV and 37 keV at E_p = 18 MeV, and a beam energy straggle of about 13 keV that is nearly independent of beam energy. The detector solid angle was about 0.15 sr and 13 to 20 cm of paraffin was inserted between the target and the NaI crystal to attenuate fast neutrons which produced an undesirable background in the detector. The resulting yield curves are shown in Fig. 2. The proton energies are computed for the center of the gas cell in the laboratory system.

The angular distributions of $^{15}N(p,\gamma_0)^{16}O$ were measured between 32° (in some cases 22° or 39°) and 135° at five to eight angles. The energy range covered was E_p = 8.6 to 18.0 MeV, in the following steps: from 8.6 to 13.65 MeV in 100 keV steps, with a few larger or smaller steps; from 14 to 17 MeV in 250 keV steps, and from 17 to 18 MeV in 125 keV steps. The gas pressures were about 0.40 Torr (2.4 mg/cm^2) corresponding to thicknesses varying from 91 keV at E_p = 10 MeV to 58 keV at E_p = 18 MeV. The detector solid angle was about 0.05 sr and 20 to 40 cm of paraffin was used between the target and detector. The 90° measurements in this series are shown in Fig. 2 for comparison with the 90° yield curves.

III. RESULTS

The measured angular distributions were fitted with the expression

$$W(E,\theta) = A_0(E)\left[1 + \sum_{n=1}^{N} a_n P_n(\cos\theta)\right] \quad (1)$$

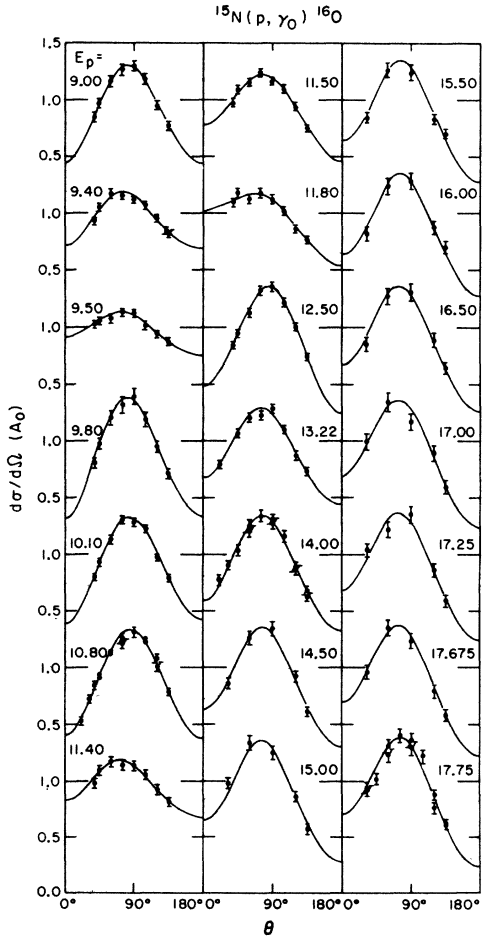

FIG. 3. Selected angular distribution measurements from $^{15}N(p,\gamma_0)^{16}O$, plotted in units of A_0.

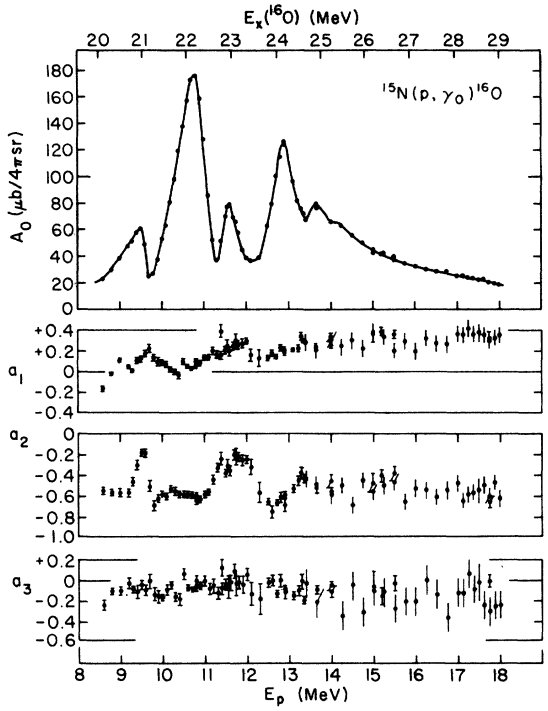

FIG. 4. Plot of A_0, a_1, a_2, and a_3 obtained from Legendre polynomial fits (k = 3) to the measured angular distributions of $^{15}N(p,\gamma_0)^{16}O$.

for N = 2, 3, and 4. Selected angular distributions plotted in units of A_0 along with the N = 3 fits are shown in Fig. 3. (For the five point angular distributions above Ep = 14 MeV, "smoothed" values of the coefficients a_1, a_2, and a_3, taken from smooth curves drawn through the points of Fig. 4, were used to obtain the curves that are compared with the data.)

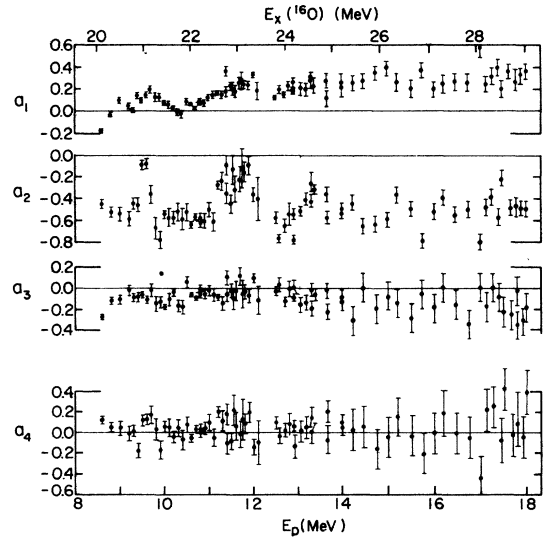

FIG. 5. Plot of a_1, a_2, a_3, and a_4 obtained from Legendre polynomial fits (k = 4) to the measured angular distributions of $^{15}N(p,\gamma_0)^{16}O$.

The total yield A_0 and angular-distribution coefficients obtained from the N = 3 fits are shown in Fig. 4. The errors indicated are statistical; those for A_0 are smaller than the data points. In this figure a distinction is made between data obtained from angular distributions measured at six to eight angles (errors with bars) and data from measurements at five angles (errors without bars).

Figure 5 shows the coefficients obtained from N = 4 fits. We note that the trends in a_1, a_2, and a_3 with energy remain the same as for the N = 3 fits. The coefficient a_4 averages nearly to zero, the fluctuations being generally within the limits of statistical error. Hence we conclude that a_4 is uniformly close to zero in this energy range with an error of about ± 0.1.

Corrections arising from the conversion of the angular distributions from laboratory to center-of-mass coordinates are considerably smaller than the statistical errors and hence were neglected. The corrections for the linear extent of the target in the gas cell are of the order of b^2, where b is the ratio of one-half the target extension to the detector distance. For our measurements b = 2.5/63.5, so b^2 = 0.0016; hence these corrections may safely be ignored. The corrections for the finite solid angle are given by Rose[39] and, even though smaller than the statistical errors, were applied to the results.

The structures in the yield as a function of energy can be seen in the 90° yield curves of Fig. 2 and in the total yield curve of A_0 shown in Fig. 4. The well-known peaks at E_x = 20.9, 22.15, 22.9, and 24.15 MeV are seen, as well as structure at 24.85. Above 25.4 MeV the yield falls smoothly.

The angular distribution coefficients show a general trend similar to that seen in other light nuclei: a_1 is positive and shows some structure but gradually increases with energy; at E_x = 21 MeV and in the range 22.5 to 24.5 MeV a_2 displays striking structure but elsewhere it is fairly constant at a value of about -0.55 which is similar to the value in most light nuclei; and a_3 is slightly negative and slowly increases in amplitude with energy.

Table 1 lists our value of the cross section of $^{15}N(p,\gamma_0)^{16}O$ measured at the peak of the strongest resonance, after conversion to the corresponding cross-section for $^{16}O(\gamma,p_0)^{15}N$ by detailed balance. The statistical error is quite small. The absolute error was determined by several measurements at 22.14 MeV and at other energies, which all agreed within ± 4%, but the overall absolute cross section accuracy is estimated at ± 20% and is due primarily to uncertainties in the line-shape analysis, with smaller contributions from uncertainties in the knowledge of the target gas pressure, solid angle, and the absorption produced by the material between the

TABLE I. Comparison of total cross-section measurements on the peak of the GDR (E_X = 22.15 MeV) in $^{16}O(\gamma,p_0)^{15}N$ and $^{16}O(\gamma,n_0)^{15}O$.

Reaction	σ^a (mb)	Reference
$^{15}N(p,\gamma_0)^{16}O$	12.9	Present work
$^{15}N(p,\gamma_0)^{16}O$	8.0	24
$^{16}O(\gamma,p_0)^{15}N$	10.7	23
$^{16}O(\gamma,p_0)^{15}N$	12.6	22
$^{16}O(\gamma,n_0)^{15}O$	5.6[b]	20
$^{16}O(\gamma,n_0)^{15}O$	7.2	19
$^{16}O(\gamma,n_0)^{15}O$	9.3[b]	18
$^{16}O(\gamma,n_0)^{15}O$	10.1	21
$^{16}O(\gamma,n_0)^{15}O$	7.2	40

[a]It is not possible to give errors for these measurements on a consistent basis. Our own estimate is that the errors lie in the range ± 20-30%.

[b]Obtained from a 90° differential measurement, using the angular distribution measured later in (γ,n_0), see Fig. 9.

target and the NaI crystal. A comparison with values from other experiments is shown in the table. Our cross section of $^{16}O(\gamma,p_0)^{15}N$ integrated between 20 and 29 MeV is 37 mb·MeV which represents 15% of the Thomas-Reiche-Kuhn sum rule.

IV. COMPARISON WITH OTHER MEASUREMENTS

Figure 6 compares our results with the measurements of Earle and Tanner[24] on $^{15}N(p,\gamma_0)^{16}O$. The two experiments are in quite good agreement. However, the better statistics and closer spacing of the present angular distribution measurements give a much more detailed picture of the variations with energy as is evident from a comparison of the solid and dashed curves.

Figure 7 compares the present results converted to $^{16}O(\gamma,p_0)^{15}N$ with the measurements of Stewart et al.,[23] which include some non-ground-state proton transitions in the data below $E_X \approx 27$ MeV. The overall trends of the two sets of data agree well. However, below 25 MeV there are differences in the amplitudes of the variations of A_0 and a_2, especially in regions where there is sharp structure and where the (γ,p_0) yield is small. It is possible that these discrepancies are due to the presence of non-ground-state protons in the work of Ref. 23. Above 25 MeV the A_0, a_1, a_2, and a_3 measurements agree within statistics.

Figure 8 compares our results with measurements of Baglin and Thompson[22] on

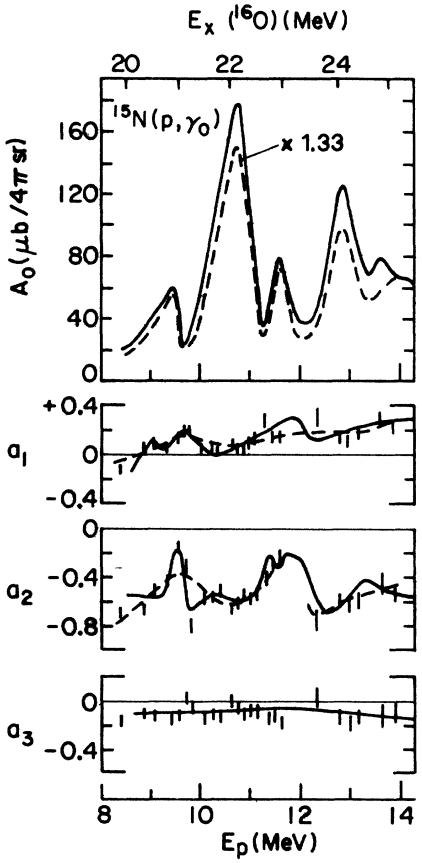

FIG. 6. The results of this experiment on $^{15}N(p,\gamma_0)^{16}O$ (solid curves) compared with those of Earle and Tanner[24] (data points and dashed curves). To facilitate comparison the A_0 curve of Ref. 24 has been multiplied by 1.33.

$^{16}O(\gamma,p_0)^{15}N$. The total yield curves agree very well. In the E_X = 21 → 25 MeV range the variations in the values of a_2 agree in amplitude and extent, although somewhat shifted in energy. Above E_X = 25 MeV their average value of a_2 is more negative than ours by about 0.1, but within statistics both curves agree in showing the same weak variations.

Figure 9 compares our results for $^{16}O(\gamma,p_0)^{15}N$ with the measurements of Jury et al.[21] on $^{16}O(\gamma,n_0)^{15}O$. The A_0 curve of (γ,n_0) shows the same structure as (γ,p_0) but does not drop off as much at higher energies. (In other (γ,n_0) measurements[18] the downward trend at higher energies agrees quite well with the (γ,p_0) data.) The trends of the two a_1 curves agree rather well but for (γ,p_0) the curve displays more structure. The two a_2 curves show structure in approximately the same regions but below 22 and above 25 MeV, the trends in the curves are quite different. For a_3 the neutron curve appears to show marked structure and on the average to be positive, in contrast to the proton curve. The (γ,n_0) results of Syme and Crawford[40]

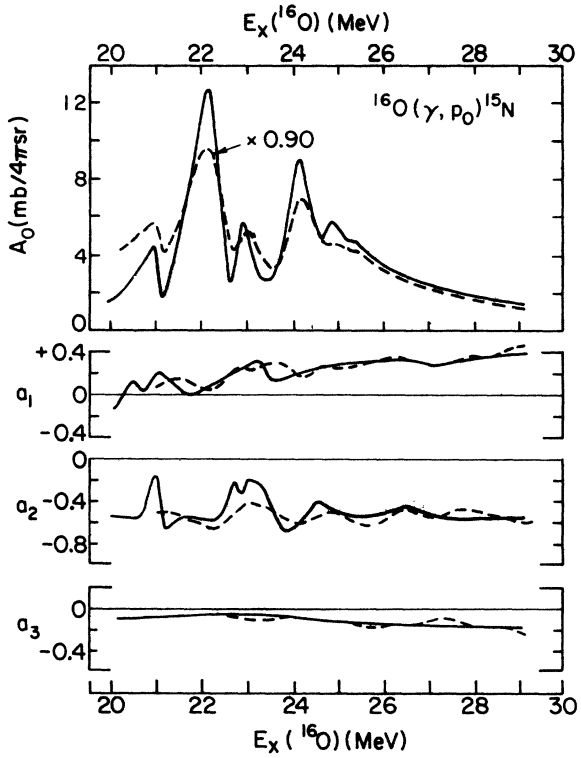

FIG. 7. The results of this experiment converted to $^{16}O(\gamma,p_0)^{15}N$ compared with those of Stewart et al.[23] (dashed curves). The A_0 curve of Ref. 23 has been multiplied by 0.90.

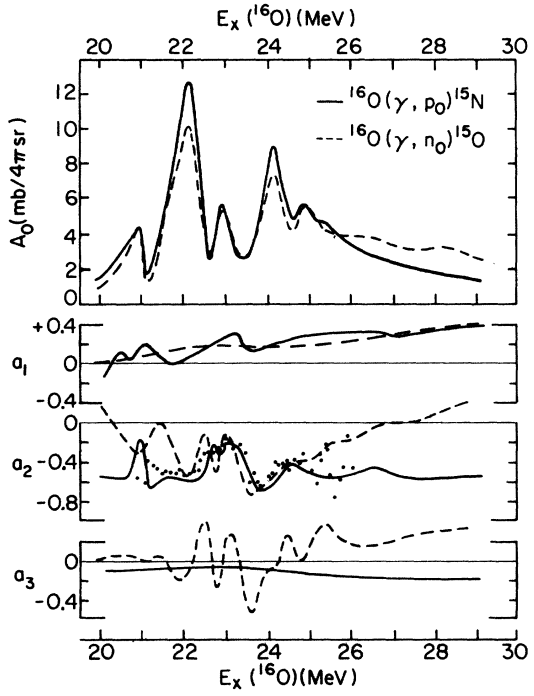

FIG. 9. The results of this experiment converted to $^{16}O(\gamma,p_0)^{15}N$ (solid curves) compared to the $^{16}O(\gamma,n_0)^{15}O$ results of Jury et al.[21] (dashed curves). The a_2 data (points) of Syme and Crawford[40] are also shown.

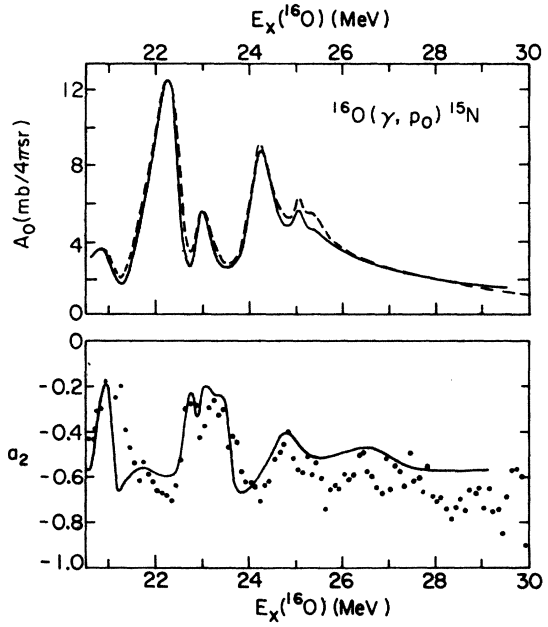

FIG. 8. The A_0 and a_2 data of this experiment converted to $^{16}O(\gamma,p_0)^{15}N$ compared with those of Baglin and Thompson.[22]

agree much more with the (γ,p_0) data than with the (γ,n_0) results of Ref. 21. This is apparent in the a_2 data given in Fig. 9.

V. STRUCTURE IN THE DIPOLE STRENGTH

The most striking aspect of the angular distribution measurements presented here is the way in which the structure in the a_2 curve correlates with the structure observed in the total yield. At E_x = 21 MeV both A_0 and a_2 show a marked interference effect and again in the region E_x = 22.5 → 25 MeV both quantities display prominent structure. Since both a_2 and A_0 are dominated by E1 radiation, these correlations support the suggestion[7] that the structure can be attributed to interference between the basic 1p-1h strength of the GDR and narrow np-nh configurations of the same spin and parity.

The basis for this model of the GDR in ^{16}O lies in the observation of narrow resonances in the reactions $^{12}C(\alpha,\gamma_0)^{16}O$ [Refs. 27,28], $^{14}N(d,\gamma)^{16}O$ [Ref. 30], and $^{13}C(^3He,\gamma_0)^{16}O$ [Ref. 29], which are correlated quite well with the structures in $^{15}N(p,\gamma_0)^{16}O$ as shown in Fig. 10. Thus, the structures in the A_0 and a_2 curves at E_x = 21 MeV are attributed to an "alpha-state" interfering with the basic 1p-1h configuration of the GDR, those at 22.7 MeV to a "deuteron-state" interference, and the

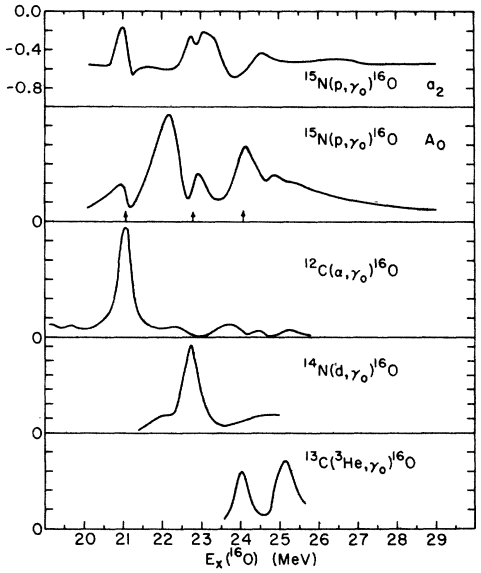

FIG. 10. Structures in the reactions $^{12}C(\alpha,\gamma_0)^{16}O$ (Refs. 27,28), $^{14}N(d,\gamma_0)^{16}O$ (Ref. 30), and $^{13}C(^3He,\gamma_0)^{16}O$ (Ref. 29) compared with the structures in A_0 and a_2 of the present experiment.

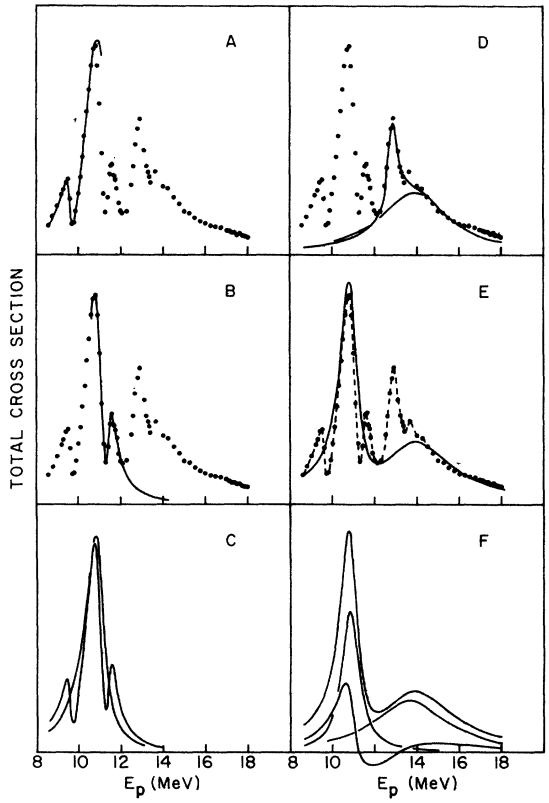

FIG. 11. Decomposition of the GDR of $^{15}N(p,\gamma_0)^{16}O$ into two main peaks and three narrower, secondary peaks. The various stages of the decomposition are explained in the text.

TABLE II. Parameters of the five states used to fit the structure in the GDR of ^{16}O.

E_x (MeV)	Γ (MeV)	$\Gamma_p\Gamma_\gamma/\Gamma$ (eV)
20.95 ± 0.01	0.32 ± 0.01	21 ± 1
22.15 ± 0.01	0.73 ± 0.01	488 ± 20
22.89 ± 0.01	0.32 ± 0.01	69 ± 5
24.07 ± 0.03	0.59 ± 0.04	130 ± 13
25.12 ± 0.06	3.15 ± 0.32	651 ± 117

peaks in the 24 → 25 MeV range to the influence of "^{3}He-states".

It can be demonstrated that this picture can produce a good empirical fit to the GDR of ^{16}O. The model assumes two "broad" resonances at $E_x \simeq 22$ and 25 MeV which interfere with each other; three "narrow" resonances at about 21, 23, and 24 MeV are then allowed to interfere with the broad resonances but are narrow enough not to interfere with each other. Various stages in the analysis, based on a standard two-state interference calculation, are illustrated in Fig. 11. In Fig. 11(A) the two interfering levels at E_x = 20.95 (narrow) and 22.15 MeV (broad) are fitted to the data. Figure 11(B) shows the fit based on the levels at E_x = 22.15 (broad) and 22.89 MeV (narrow). These fits are combined in Fig. 11(C) to show the resulting broad resonance at 22.15 MeV and the actual observed curve. Fig. 11(D) shows the fit obtained with the two levels at 24.07 (narrow) and 25.12 MeV (broad), along with the latter resonance itself. The dashed curve in Fig. 11(E) shows the final fit to the data resulting from the five-level model. The solid curve shows the contribution from the two broad levels alone, which are presumed to represent the main GDR. In Fig. 11(F) this curve is decomposed into its constituents: the two resonances acting alone and the interference between them. The resonance parameters obtained from these fits are listed in Table II.

Recently, a two-state model has been applied by Kabachnik and Razuvaev[41] to explain the interference effect seen in the coefficient a_2 at E_x = 21 MeV. They find that fairly good agreement can indeed be obtained with the observed effect. On a more formal basis Shakin and Wang[8] have applied the doorway state model[42] to explain the structure in the reaction $^{16}O(\gamma,n_0)^{15}O$ which is very similar to that in $^{16}O(\gamma,p_0)^{15}N$ (see Fig. 9). In this calculation, however, they invoke 3p-3h states for all of the interfering states.

VI. CONFIGURATIONS OF THE GDR

If we accept the picture discussed in Section V, then the GDR of ^{16}O consists of two dominant E1 resonances, the remaining structures being attributable to inter-

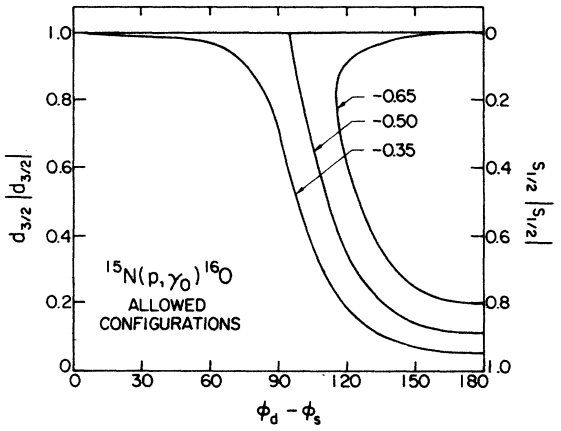

FIG. 12. Configurations in $^{15}N(p,\gamma_0)^{16}O$ allowed by the angular distributions a_2 = -0.35, -0.50, and -0.65. The curves define the relationship between the intensity $d_{3/2}|d_{3/2}|$ and the phase difference $\phi_d - \phi_s$.

ferences with np-nh states which presumably carry only a small fraction of the E1 strength. If we are interested in determining the configurations in the p_0 channel which form these two basic resonances, we may consider only the a_2 coefficient which, for a $J^\pi = 1/2^-$ target nucleus, is given by

$$a_2 = -0.50(d_{3/2})^2 + 1.414(d_{3/2})(s_{1/2})\cos(\phi_d-\phi_s), \quad (2)$$

where $s_{1/2}e^{i\phi_s}$ and $d_{3/2}e^{i\phi_s}$ are the complex amplitudes of the allowed proton waves normalized to

$$(s_{1/2})^2 + (d_{3/2})^2 = 1. \quad (3)$$

The allowed solutions for values of a_2 = -0.35, -0.50, and -0.65 are shown in Fig. 12. From Fig. 4 we see that the experimental values of a_2 lie well within this range (except for the excursions attributed to interference effects) with an average value of about -0.55. Although this value severely restricts the possible solutions, nevertheless, it is possible for the relative amounts of s and d wave to vary all the way from nearly pure d wave to predominantly s wave in different parts of the GDR, although a constant solution is of course allowed. Measurements with polarized protons would produce definitive solutions.[34]

It has been customary to identify the two broad resonances in this model with the two lp-1h configurations which carry the major portion of E1 strength in the calculations,[3] as shown in Table III. We see that this identification attributes the splitting of the GDR in ^{16}O to a spin-orbit splitting and confirms that a significant amount of dipole strength resides in the spin-flip configuration $p_{3/2}^{-1}d_{3/2}$.

It is clear that, whatever solutions are obtained for the proton channel, they cannot match directly these particle-hole configurations of the GDR. The former consist of a $(d_{3/2},s_{1/2})$ proton and a $J^\pi = 1/2^-$ nucleus ^{15}N (mainly $p_{1/2}^{-1}$), while the latter are predominantly $(d_{5/2},d_{3/2})p_{3/2}^{-1}$. Despite this mismatch the proton and neutron channels account for a significant portion of the E1 sum rule (Section III). Clearly, there must exist a natural mechanism for passing from the continuum state to the dipole state. Such a mechanism can be found in the doorway-state model[42] which has been successfully applied to this problem.[8,43]

It is of course possible that the GDR of ^{16}O consists of a single coherent resonance throughout which the configuration does not vary. This would be the case if the spin-orbit splitting in the force which produces the two levels discussed above was very small. Recent calculations of the GDR in ^{16}O have in fact given such a single coherent resonance.[44] In this case it might be possible to attribute the apparent formation of the two broad resonances from a single resonance to the effect of an interference with a complex structure in much

TABLE III. Configurations of the dipole states in ^{16}O from Ref. 3.[a]

E_x MeV	$p_{1/2}^{-1}s_{1/2}$	$p_{1/2}^{-1}d_{3/2}$	$p_{3/2}^{-1}s_{1/2}$	$p_{3/2}^{-1}d_{5/2}$	$p_{3/2}^{-1}d_{3/2}$	Strength %
13.7	1.00	-0.02	-0.06	-0.02	0.02	1
17.6	0.01	0.90	-0.09	-0.38	-0.21	1
20.0	0.06	-0.02	0.96	-0.24	-0.08	1
22.2	0.04	0.35	0.20	0.90	-0.20	68
25.0	-0.01	0.27	0.10	0.09	0.95	29

[a]A zero-range force with a Soper mixture is used.

the same way as the finer structure was explained in this manner. It has also been suggested that the splitting might be due to deformation effects in the excited ^{16}O nucleus.[45]

VII. EVIDENCE FOR GIANT QUADRUPOLE STRENGTH

The presence of the term $a_1P_1(\cos\theta)$ in the measured angular distributions indicates interference between the dominant E1 strength and either M1 or E2 radiation or both. On the other hand, the presence of a term $a_3P_3(\cos\theta)$ arises only from E2-E1 interference. In Figs. 4 and 5 we see that a non-zero value of a_3 is established in the region studied, thus establishing the presence of E2 radiation throughout the region of the GDR in ^{16}O.

Frederick et al.[23] have carried out a detailed analysis of their results on $^{16}O(\gamma,p_0)^{15}N$ illustrated in Fig. 7 to obtain the E2 cross section between E_γ = 21 and 33 MeV. A plausible assumption was made for the phase difference between the E1 and E2 amplitudes. They found E2 strength rising from 21 MeV to a maximum at about 26 MeV and then a slowly falling plateau to 33 MeV. This calculation constituted the first definite identification of an E2 giant resonance in nuclei, although earlier angular distribution measurements in (p,γ) reactions had definitely identified the presence of E2 strength. The present results, in essential agreement with those of Ref. 23 (see Fig. 7), confirm the presence of this E2 strength in ^{16}O, although definitive results were not obtained until measurements were made with the polarized $(\vec{p},\gamma)$ reaction.[34]

VIII. OTHER REACTIONS

In the course of this experiment, information was obtained on other reactions. An unresolved group of capture gamma rays corresponding to transitions to the four excited states of ^{16}O at 6.05, 6.13, 6.92, and 7.12 MeV were observed. Figure 13 shows the yield curve obtained for these unresolved gamma rays. It is interesting to note the emergence of a giant structure in the region E_x = 24 to 29 MeV. The angular distributions indicate typical dipole raditaion. This structure lies about 4 MeV above the ground-state GDR. Thus, the excitation energy of the E1 strength built upon excited states in ^{16}O appears to be somewhat less than that of the ground state. The structure observed in the γ_{1-4} curve agrees well with that obtained in

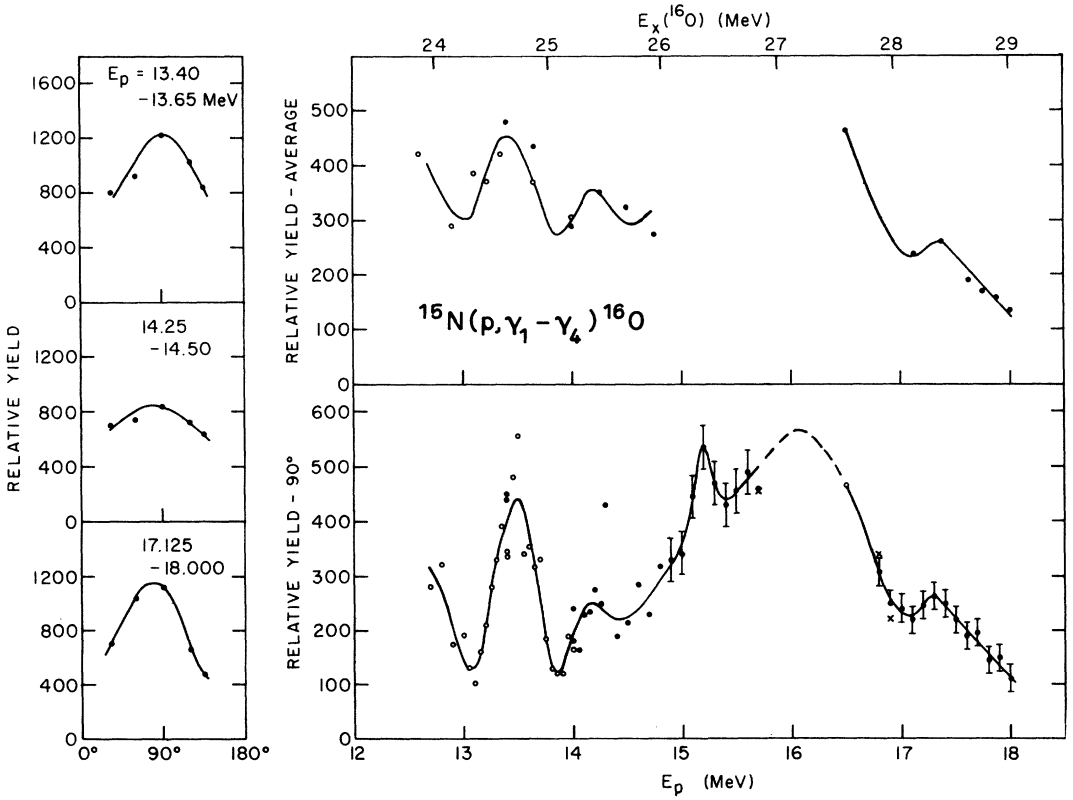

FIG. 13. Yield of $^{15}N(p,\gamma_1-\gamma_4)^{16}O^*$. Top right: data integrated over the angular distribution measurements. Bottom right: 90° data; below E_p = 15 MeV different symbols indicate different analyses. Left: angular distributions summed over the energy intervals indicated.

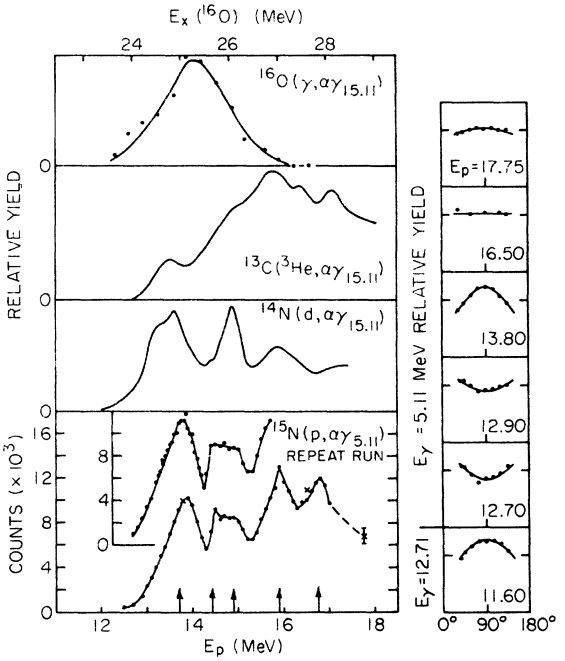

FIG. 14. Left: The 90° yield of $^{15}N(p,\alpha\gamma_{15.11})^{12}C$ compared with other reactions leading to the same decay of ^{16}O (Refs. 47-49). Right: angular distributions of the 15.11-MeV γ-ray at several energies and the 12.71-MeV γ-ray at one energy.

the $\gamma_{1,2}$ curve by Chew et al.[46] Moreover, these authors find most of the structure is due to the γ_2 transitions to the 3^- level at 6.13 MeV and they discuss possible interpretations of this structure.

The particle reaction $^{15}N(p,\alpha\gamma_{15.11})^{12}C$ leads to the strong production of 15.1-MeV gamma rays above the threshold. The yield obtained for this reaction is given in Fig. 14 and compared with other reactions[47-49] having the same exit channel but different input channels. There appears to be some correspondence in the structures (indicated by the arrows) appearing in the reactions initiated by particles, but the photoexcitation has an entirely different appearance. This undoubtedly reflects the selective excitation of dipole strength in the photoexcitation process.

Angular distributions obtained for the 15.1-MeV gamma rays from $^{15}N(p,\alpha\gamma_{15.1})^{12}C$ are also shown in Fig. 14, along with one for the 12.71-MeV gamma ray resulting from feeding the 12.71-MeV state of ^{12}C. Since these gamma rays deexcite a single level of fixed spin and parity (1^+), the angular distributions must be symmetric about 90°. Thus, the symmetric nature of these angular distributions provides a good test of the quality of the angular distribution measurements. The striking variation in these angular distributions as compared to those of the $^{15}N(p,\gamma)^{16}O$ reactions again emphasizes the remarkable constancy of the latter distributions resulting from the selective nature of the photon channel and the dominating characteristics of the GDR itself.

Note added in proof: Chewe et al. [Nucl. Phys. A 286, 451 (1977)] have measured A_0, a_1. . . a_4 for $^{15}N(p,\gamma_0)^{16}O$ from E_p = 6 to 21 MeV with results generally in agreement with those in this paper. However, the angular distributions are not detailed enough to reveal all the structure observed in the present experiment.

We would like to thank J. L. Black and G. L. Latshaw for their participation in the early stages of this work. This work was supported in part by the U.S. National Science Foundation.

*Present address: EDS Nuclear Inc., 220 Montgomery St., San Francisco, CA 94104.

[1] D. H. Wilkinson, Physica 22, 1039 (1956).
[2] J. P. Elliott and B. H. Flowers, Proc. Roy. Soc. 241, 57 (1957).
[3] G. E. Brown, L. Castillejo, and J. A. Evans, Nucl. Phys. 22, 1 (1961).
[4] B. Buck and A. D. Hill, Nucl. Phys. A95, 271 (1967).
[5] A. M. Saruis and M. Marangoni, Nucl. Phys. A132, 433 (1969).
[6] J. D. Perez and G. J. Stephenson, Jr., Nucl. Phys. A165, 152 (1971).
[7] V. Gillet, M. A. Melkanoff, and J. Raynal, Nucl. Phys. A97, 631 (1967).
[8] C. M. Shakin and W. L. Wang, Phys. Rev. Lett. 26, 902 (1971).
[9] G. E. Walker, Phys. Rev. 174, 1290 (1968).
[10] A. Agodi, M. Baldo, and F. Catara, Nucl. Phys. A171, 199 (1971).
[11] L. L. Foldy and J. D. Walecka, Nuovo Cimento 34, 1026 (1964).
[12] J. D. Murphy, R. Raphael, H. Überall, R. F. Wagner, D. K. Anderson, and C. Werntz, Phys. Rev. Lett. 19, 714 (1967).
[13] I. Sick, E. B. Hughes, T. W. Donnelly, J. D. Walecka, and G. E. Walker, Phys. Rev. Lett. 23, 1117 (1969).
[14] H. W. Baer, K. M. Crowe, and P. Truöl, in Advances in Nuclear Physics, eds. M. Baranger and E. Vogt (Plenum Press, N.Y., 1976) Vol. 9.
[15] J. B. Seaborn, Phys. Rev. 179, 958 (1969).
[16] B. S. Dolbilkin, V. I. Korin, L. E. Lazareva, and R. A. Nikolaev, Zh. Eksp. Teo. Fiz. 1, 47 (1965). [Sov. Phys. - JETP Lett. 1, 148 (1965).]
[17] J. Ahrens et al., in Proc. Int. Conf. on Photonuclear Reactions and Applications, Asilomar, ed. B. L. Berman (Lawrence Livermore Laboratory, Livermore, 1973) Vol. I, p. 23.
[18] C. P. Wu, F. W. K. Firk, and T. W. Phillips, Phys. Rev. Lett. 20, 1182 (1968).
[19] J. T. Caldwell, R. L. Bramblett, B. L.

Berman, R. R. Harvey, and S. C. Fultz, Phys. Rev. Lett. 15, 976 (1965).
[20]V. V. Verbinski and J. C. Courtney, Nucl. Phys. 73, 398 (1965).
[21]J. W. Jury, J. S. Hewitt, and K. G. McNeill, Canad. J. Phys. 48, 1635 (1970).
[22]J. E. E. Baglin and M. N. Thompson, Nucl. Phys. A138, 73 (1969).
[23]R. J. J. Stewart, R. C. Morrison, and D. E. Frederick, Phys. Rev. Lett. 23, 323 (1969); D. E. Frederick, R. J. J. Stewart, and R. C. Morrison, Phys. Rev. 186, 992 (1969).
[24]E. D. Earle and N. W. Tanner, Nucl. Phys. A95, 241 (1967).
[25]J. L. Black, W. J. O'Connell, S. S. Hanna, and G. L. Latshaw, Phys. Lett. 25B, 405 (1967).
[26]J. T. Caldwell, S. C. Fultz, and R. L. Bramblett, Phys. Rev. Lett. 19, 447 (1967).
[27]M. Suffert and W. Feldman, Phys. Lett. 24B, 579 (1967).
[28]K. A. Snover, E. G. Adelberger, and D. R. Brown, Phys. Rev. Lett. 32, 1061 (1974).
[29]N. G. Puttaswamy and D. Kohler, Phys. Lett. 20, 288 (1966).
[30]M. Suffert, Nucl. Phys. 75, 226 (1965).
[31]R. G. Allas, S. S. Hanna, L. Meyer-Schützmeister, R. E. Segel, P. P. Singh, and Z. Vager, Phys. Rev. Lett. 13, 628 (1964); R. A. Ferrell and W. M. MacDonald, Phys. Rev. Lett. 16, 187 (1966).
[32]N. W. Tanner, Nucl. Phys. 63, 383 (1965).
[33]G. Dearnaley, D. S. Gemmell, B. W. Hooten, and G. A. Jones, Nucl. Phys. 64, 177 (1965).
[34]S. S. Hanna, H. F. Glavish, R. Avida, J. R. Calarco, E. Kuhlmann, and R. LaCanna, Phys. Rev. Lett. 32, 114 (1974).
[35]K. Shoda, Nucl. Phys. 72, 305 (1965).
[36]D. F. Measday, A. B. Clegg, and P. S. Fisher, Nucl. Phys. 61, 269 (1965).
[37]H. M. Kuan, M. Hasinoff, W. J. O'Connell, and S. S. Hanna, Nucl. Phys. A151, 129 (1970).
[38]M. Suffert, W. Feldman, J. Mahieux, and S. S. Hanna, Nucl. Instr. and Meth. 63, 1 (1968).
[39]M. E. Rose, Phys. Rev. 91, 610 (1953).
[40]D. B. C. B. Syme and G. I. Crawford, in Proc. Int. Conf. on Photonuclear Reactions and Applications, Asilomar, ed. B. L. Berman (Lawrence Livermore Laboratory, Livermore, 1973) Vol. II, p. 1055.
[41]N. M. Kabachnik and V. N. Razuvaev, Phys. Lett. 61B, 420 (1976).
[42]H. Feshbach, A. K. Kerman, and R. H. Lemmer, Ann. of Phys. (N.Y.) 41, 230 (1967).
[43]D. G. Mavis, Ph.D. dissertation, Stanford University, 1977 (unpublished).
[44]S. Krewald, V. Klemt, J. Speth, and A. Faessler, Nucl. Phys. A281, 166 (1977).
[45]J. S. O'Connell (private communication).
[46]S. H. Chew, J. Lowe, J. M. Nelson, and A. R. Barnett, Nucl. Phys. A229, 241 (1974).
[47]J. T. Caldwell, Ph.D. dissertation, University of California, 1967 (unpublished).
[48]C. P. Browne, I. F. Wright, and W. A. Schier, Nucl. Phys. 66, 49 (1965).
[49]H. R. Weller, H. A. van Rinsvelt, and F. E. Dunham, Phys. Lett. 27B, 283 (1968).